



LAWRENCE
LIVERMORE
NATIONAL
LABORATORY

Multi-Scale, Multi-Physics Membrane Technology

W. D. Henshaw

February 23, 2009

Disclaimer

This document was prepared as an account of work sponsored by an agency of the United States government. Neither the United States government nor Lawrence Livermore National Security, LLC, nor any of their employees makes any warranty, expressed or implied, or assumes any legal liability or responsibility for the accuracy, completeness, or usefulness of any information, apparatus, product, or process disclosed, or represents that its use would not infringe privately owned rights. Reference herein to any specific commercial product, process, or service by trade name, trademark, manufacturer, or otherwise does not necessarily constitute or imply its endorsement, recommendation, or favoring by the United States government or Lawrence Livermore National Security, LLC. The views and opinions of authors expressed herein do not necessarily state or reflect those of the United States government or Lawrence Livermore National Security, LLC, and shall not be used for advertising or product endorsement purposes.

This work performed under the auspices of the U.S. Department of Energy by Lawrence Livermore National Laboratory under Contract DE-AC52-07NA27344.

FY08 LDRD Feasibility Study Final Report
Multi-Scale, Multi-Physics Membrane Technology
LDRD Project Tracking Code: 08-FS-016
William D. Henshaw, Principal Investigator

Abstract

Our objectives for this 10 week feasibility study were to gain an initial theoretical understanding of the numerical issues involved in modeling fluid-structure interface problems and to develop a prototype software infrastructure based on deforming composite grids to test the new approach on simple problems. For our first test case we considered a two-dimensional fluid-solid piston problem in which one half of the domain is occupied by fluid and the other half by a solid. We determined the exact solution to this problem using the method of characteristics and d'Alembert's solution to the wave equation. We solved this problem using our new numerical approximations and verified the results compared to the exact solution. As a second test case we considered a two dimensional problem consisting of a shock in a fluid that strikes a cylindrically shaped solid.

Contents

1	Introduction/Background	3
2	Research Activities and Results	3
2.1	The Overlapping Grid Approach for Multi-Domain Problems	4
2.2	Governing equations	6
2.3	A fluid-solid piston problem	7
2.3.1	Solution for the fluid	7
2.3.2	Solution for the solid	8
2.3.3	Solution to the coupled fluid-solid problem	10
2.3.4	Initial conditions of a solid at rest	10
2.3.5	Solid initial conditions chosen to give a specified fluid motion	11
2.3.6	Fluid-solid piston problem results	11
2.4	The FSI-DCG numerical approach	11
3	Exit Plan	12
4	References	13

1 Introduction/Background

There are many important multi-physics problems that require the simulation of a gas or fluid coupled to the motion of deforming solids. These include applications from DOD (weapons effects, insensitive munitions, warhead design, composite armor, and earth penetration), DOE (vibrations in reactor fuel rods for GNEP, NIF holhraum targets), DHS (threat assessment and neutralization), and industry (ablation, fluidized beds, combustion, pharmaceutical). It is difficult for one algorithm to efficiently and accurately treat all the different phases (gas, liquid, solid) and existing simulation codes are limited in their ability to solve problems in this class. We propose the development of a general purpose interface coupling technology called "membranes" that can be used to couple two different physics solvers. The physics solvers will in general solve different equations, on different grids with different numerical approximations. The membrane technology will serve as the agent that couples the disparate grids and solves the interface matching conditions that, for example, impose continuity and stress jump conditions. The Overture project in CASC has developed an efficient gas-phase reacting flow solver (CGCNS) that use moving overlapping grids and adaptive mesh refinement to model shocks and detonations. The ALE3D solver from B-division can effectively model the deformation of a wide class of solids. The longer term goal of this project will focus on coupling the Overture compressible flow solver, CGCNS, and ALE3D. The membrane technology will also be applicable for coupling other physics solvers (e.g. DIABLO). The resulting coupled multi-physics solver will enable the simulation of some very difficult but important problems and generate the interest and potential new funding from the DOD, DHS, DTRA, as well as industry.

The objectives of this 10 week feasibility study are two-fold. The first is to gain an initial theoretical understanding of some of the numerical issues involved in modeling fluid-structure problems and the second is to begin development of the membrane software-infrastructure while testing the approach on some simple problems. On the theoretical side we will analyze and develop methods for solving the one-dimensional interface model problem that couples a fluid in one half of the domain with a solid in the other half. Here we will consider the problems of well-posedness of the problem and interface conditions, and the stability and accuracy of discrete approximations. The question of developing higher-order accurate approximations will be considered. Time-stepping algorithms will be developed for treating the case when the characteristic wave speeds of the fluid and solid are widely different. On the development side, we will construct a prototype version of the membrane software infrastructure for treating multi-dimensional interfaces and use this infrastructure to solve some simple two-dimensional fluid-structure problems. The first target example will consider a two-dimensional problem where one half the domain is occupied by fluid and the other half by a solid. A shock sent through the fluid will impinge on the solid region, causing reflected and transmitted waves and causing the solid to deform. The grid in the fluid and the grid in the solid will deform. We will use fluid flow solvers from Overture coupled to a simple solid-mechanics code. The second target example will consider a fluid coupled to a solid of more general shape such as a cylinder or ellipsoid.

2 Research Activities and Results

We have developed a numerical approach for modeling fluid-structure problems. We have designed and begun development of a software infrastructure for modeling multi-physics multi-domain problems. Different physics solvers (e.g. compressible flow solver or solid-mechanics solver) are associated with each domain. The approach is based on the use of moving overlapping grids and accurate approximations to the interface jump conditions.

We have analysed the problem of a fluid domain separated from a solid domain by a moving planar interface. An exact solution to this problem was determined in the case when the fluid is governed by the Euler equations and the solid is governed by linear elasticity. The solution to this problem was computed with our new approach and the exact solution was used to measure the error. We have also demonstrated the approach for solving an elastic cylinder embedded in a fluid.

We have analysed the numerical stability and accuracy of new centered interface approximation for the jumps in temperature and heat flux at the fluid-solid interface and have published a paper describing this approach [7].

2.1 The Overlapping Grid Approach for Multi-Domain Problems

In this section we describe the basic features of the overlapping grid approach for solving multi-domain problems. We are interested in finding the solution $\mathbf{u}(\mathbf{x}, t)$ to a PDE initial-boundary-value problem in a deforming domain Ω ,

$$\begin{aligned}\mathcal{L}(\mathbf{u}, \partial_t \mathbf{u}, \partial_{x_\mu} \mathbf{u}) &= \mathbf{f}(\mathbf{x}, t), & \mathbf{x} \in \Omega, \\ \mathcal{B}(\mathbf{u}, \partial_t \mathbf{u}, \partial_{x_\mu} \mathbf{u}) &= \mathbf{g}(\mathbf{x}, t), & \mathbf{x} \in \partial\Omega, \\ \mathcal{I}(\mathbf{u}, \partial_t \mathbf{u}, \partial_{x_\mu} \mathbf{u}) &= \mathbf{h}(\mathbf{x}), & \mathbf{x} \in \Omega, t = 0,\end{aligned}$$

where \mathcal{L} denotes the partial differential equations, \mathcal{B} the boundary conditions and \mathcal{I} the initial conditions. For now we consider the general case; in later sections we give more specific details of the equations we solve for problem areas of particular interest. The domain Ω may consist of a set of \mathcal{N}_d sub-domains that represent different materials,

$$\Omega = \cup_{d=1}^{\mathcal{N}_d} \Omega_d . \quad (1)$$

Figure 1, for example, shows the domain for a conjugate heat transfer problem that consists of multiple fluid and solid sub-domains. As indicated by Ω_3 in the figure, a single sub-domain may be multiply connected. For multi-domain problems we will also need appropriate interface conditions that couple the solutions where sub-domains meet. Examples of these interface equations are given in later sections.

The entire domain of interest, Ω , is discretized using a composite overlapping grid, \mathcal{G} . Each fluid or solid sub-domain will itself be discretized with an overlapping grid, \mathcal{G}_d , with the global overlapping grid \mathcal{G} containing all the sub-overlapping grids,

$$\mathcal{G} = \cup_{d=1}^{\mathcal{N}_d} \mathcal{G}_d . \quad (2)$$

The overlapping grid \mathcal{G} consists of a set of $\mathcal{N}_{\text{grid}}$ component grids G_g , i.e.,

$$\mathcal{G} = \{G_g\}, \quad g = 1, 2, \dots, \mathcal{N}_{\text{grid}} .$$

The component grids cover Ω . Similarly, the overlapping grid, \mathcal{G}_d , for a sub-domain, will consist of a set of overlapping component grids which are a sub-set of the grids in \mathcal{G} . Each component grid is a logically rectangular, curvilinear grid defined by a smooth mapping \mathbf{C}_g from parameter space \mathbf{r} (e.g. the unit-cube in three dimensions) to physical space \mathbf{x} :

$$\mathbf{x} = \mathbf{C}_g(\mathbf{r}, t), \quad \mathbf{r} \in [0, 1]^3, \quad \mathbf{x} \in \mathbb{R}^3 . \quad (3)$$

For moving grids, the mapping will depend on time. The mapping is used to define the metric derivatives $\partial \mathbf{x} / \partial \mathbf{r}$ and the grid points at any desired resolution.

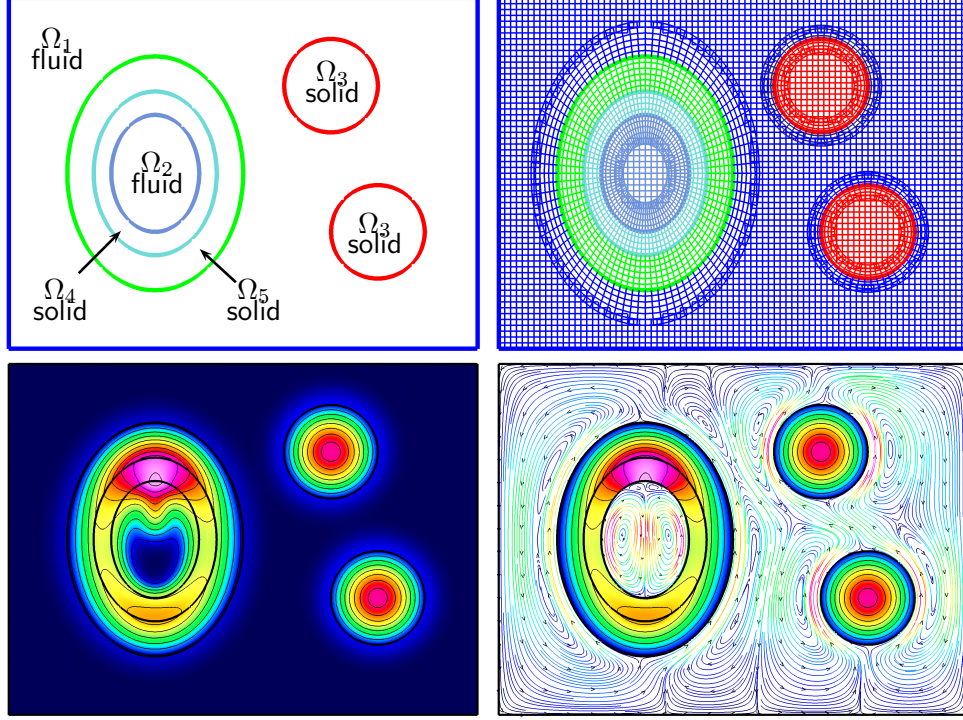


Figure 1: Top left : a domain Ω with two fluid sub-domains Ω_1, Ω_2 and three solid sub-domains Ω_3, Ω_4 and Ω_5 . Top right: the composite \mathcal{G} consists of five overlapping grids, one for each domain. Bottom left: a computed conjugate heat transfer solution showing the temperature. Bottom right: the streamlines in the fluid domains and the temperature in the solid domains.

The governing PDEs are typically discretized with a finite difference or finite volume approximation. For example, consider approximating the generalized Laplace operator, L defined by

$$Lw = \nabla \cdot (a \nabla w), \quad (4)$$

where $a = a(\mathbf{x})$ is a real valued coefficient. A straight-forward approach to discretize L on a curvilinear grid is to use the mapping method, as follows. Using the chain rule, the operator L can be written in general curvilinear coordinates in n_d space dimensions as

$$Lw = \sum_{i=1}^{n_d} \sum_{j=1}^{n_d} \sum_{k=1}^{n_d} a \frac{\partial r_k}{\partial x_i} \frac{\partial r_j}{\partial x_i} \frac{\partial^2 w}{\partial r_j \partial r_k} + \frac{\partial r_k}{\partial x_i} \left\{ a \frac{\partial}{\partial r_k} \left(\frac{\partial r_j}{\partial x_i} \right) + \frac{\partial a}{\partial r_k} \frac{\partial r_j}{\partial x_i} \right\} \frac{\partial w}{\partial r_j}. \quad (5)$$

The metric terms $\partial r_j / \partial x_k$ are computed from the mapping that defines the grid and are thus assumed to be known. The derivatives with respect to the parameter space coordinates r_j can be approximated with difference approximations. The operator L can also be written in *conservation* form, or *self-adjoint* form, in general curvilinear coordinates as

$$Lw = \frac{1}{J} \sum_{j=1}^{n_d} \sum_{k=1}^{n_d} \frac{\partial}{\partial r_j} \left(A^{jk} \frac{\partial w}{\partial r_k} \right), \quad A^{jk} = a J \sum_{\mu=1}^{n_d} \sum_{\nu=1}^{n_d} \frac{\partial r_j}{\partial x_\mu} \frac{\partial r_k}{\partial x_\nu}, \quad (6)$$

where J denotes the determinant of the Jacobian matrix $[\partial x_j / \partial r_k]$. A careful discretization of this last form of the operator leads to symmetric and compact discrete approximations of any order of

accuracy as developed in our previous work [5]. These approximations are generalized finite-volume approximations.

Solution values at interpolation points of some grid G_1 , for example, are determined by interpolation from donor points on some other grid G_2 . For each interpolation point \mathbf{x}_1 on grid G_1 , its parameter space coordinates, $\mathbf{r}_2 = \mathbf{C}_{g_2}^{-1}(\mathbf{x}_1)$, on grid G_2 may be found using the inverse mapping. In parameter space, standard tensor-product polynomial interpolation is used, such as linear interpolation (i.e., bi-linear for $n_d = 2$ or tri-linear for $n_d = 3$). For first order hyperbolic systems, such as the reactive Euler equations, linear interpolation is sufficient for second-order accuracy, while the solution of a second-order elliptic equations, such as Laplace's equation, would normally require quadratic interpolation for second-order accuracy; see the discussion in Chesshire and Henshaw [2] for further details.

In the multi-domain context we will use a partitioned approach and associate a separate physics solver with each sub-domain. The physics solver for a sub-domain will advance the solution using an explicit or implicit predictor-corrector type time-stepping algorithm. A multi-physics solver will coordinate the different domain solvers and ensure that the interface equations are satisfied. More details of our time-stepping approach as applied to conjugate heat transfer can be found in [7]. The stability and accuracy of the interface approximations and the coupled approach is of primary concern in our work.

2.2 Governing equations

We are concerned with the solution to fluid-structure problems in a domain that deforms over time. Let Ω_t denote this domain at time t . The equations of motion for the fluid and solid are governed by the equations of conservation of mass, momentum and energy, together with constitutive equations and equations of state. In a fixed Eulerian reference frame, the conservation equations for mass and momentum are

$$\frac{\partial \rho}{\partial t} + \nabla \cdot (\rho \mathbf{v}) = 0, \quad (7)$$

$$\frac{\partial(\rho \mathbf{v})}{\partial t} + \nabla \cdot (\rho \mathbf{v} \otimes \mathbf{v}) = \nabla \cdot \boldsymbol{\sigma} + \rho \mathbf{f}, \quad (8)$$

where ρ is the density, \mathbf{v} the velocity and $\boldsymbol{\sigma}$ the stress tensor. These equations can also be written in a Lagrangian frame. For our purposes, however, we consider a general (ALE) moving coordinate system, $\mathbf{x} = \mathbf{G}(\mathbf{X}, t)$, where \mathbf{X} denotes a point in the reference configuration Ω . In a numerical simulation, \mathbf{G} will be the equation of motion for the grid. In this general moving frame, the momentum equations take the form

$$\frac{\partial(\rho J_g \mathbf{v})}{\partial t} + \nabla_{\mathbf{X}} \cdot (\rho J_g \mathbf{v} \otimes (\mathbf{v} - \mathbf{v}_g) \mathbf{F}_g^{-T}) = \nabla_{\mathbf{X}} \cdot (J_g \boldsymbol{\sigma} \mathbf{F}_g^{-T}) + \rho J_g \mathbf{f}, \quad (9)$$

where $\nabla_{\mathbf{X}}$ is the divergence with respect to \mathbf{X} , $\mathbf{v}_g = \partial \mathbf{G} / \partial t$ is the *grid velocity*, $\mathbf{F}_g = \partial \mathbf{G} / \partial \mathbf{X}$ and $J_g = \det(\mathbf{F}_g)$. The momentum equations in this general frame (9) reduce to the Eulerian equations (8) or the Lagrangian equations with the appropriate choice of \mathbf{G} . The equations for the conservation of mass and energy in the general frame can be described in a similar way, see for example [1]. Using the relation $\partial J_g / \partial t = J_g \nabla \cdot \mathbf{v}_g$, equation (9) can be written in the alternative form

$$\frac{\partial(\rho \mathbf{v})}{\partial t} + \frac{1}{J_g} \nabla_{\mathbf{X}} \cdot (\rho J_g \mathbf{v} \otimes (\mathbf{v} - \mathbf{v}_g) \mathbf{F}_g^{-T}) + \rho \mathbf{v} \frac{1}{J_g} \nabla_{\mathbf{X}} \cdot (J_g \mathbf{v}_g \mathbf{F}_g^{-T}) = \frac{1}{J_g} \nabla_{\mathbf{X}} \cdot (J_g \boldsymbol{\sigma} \mathbf{F}_g^{-T}) + \rho \mathbf{f}, \quad (10)$$

which includes a source term. This latter form is sometimes preferred in numerical approximations [?] since it is easier to enforce that the solution be exact for uniform flows (the so-called *geometric conservation law*).

Fluid description: For fluid domains we will consider the solution to the inviscid compressible Euler equations, the compressible Navier-Stokes equations or the viscous incompressible Navier-Stokes equations. These different formulations are determined by the appropriate choice of constitutive laws and equations of state. For a Newtonian viscous fluid, for example, the stress tensor in (9) is $\boldsymbol{\sigma} = -p\mathbf{I} + \mu(\nabla\mathbf{v} + \nabla\mathbf{v}^T)$, where p is the pressure. In the inviscid case $\mu = 0$, while in the incompressible case $\nabla \cdot \mathbf{v} = 0$.

Solid description: In solid domains we will begin by considering small displacement linear elasticity. In this case the equations of motion are

$$\rho \frac{\partial^2 \mathbf{u}}{\partial t^2} = \nabla_{\mathbf{x}} \cdot \boldsymbol{\sigma}, \quad \boldsymbol{\sigma} = \lambda(\nabla_{\mathbf{x}} \cdot \mathbf{u}) \mathbf{I} + \mu(\nabla_{\mathbf{x}} \mathbf{u} + \nabla_{\mathbf{x}} \mathbf{u}^T), \quad (11)$$

where $\mathbf{u} = \mathbf{x} - \mathbf{X}$ is the displacement. Subsequently we will extend the approach to large-displacement and large deformation. For example, a commonly used constitutive law for small-strain and large displacement is the St. Venant-Kirchoff material

$$\mathbf{S} = \lambda \operatorname{tr}(\mathbf{E})\mathbf{I} + 2\mu, \quad \boldsymbol{\sigma} = J^{-1}\mathbf{F}(\lambda \operatorname{tr}(\mathbf{E})\mathbf{I} + 2\mu\mathbf{E})\mathbf{F}^T, \quad (12)$$

where $\mathbf{E} = \frac{1}{2}(\mathbf{F}^T\mathbf{F} - \mathbf{I})$ is the Green-Lagrange strain tensor and \mathbf{S} is the second Piola-Kirchoff stress. For large deformation, the Mooney-Rivlin material [1] is commonly used as a simple constitutive law.

Interface conditions: At a fluid-solid interface, the jump conditions are

$$[\mathbf{v}]_{\mathcal{I}} = 0, \quad [\mathbf{n} \cdot \boldsymbol{\sigma}]_{\mathcal{I}} = 0, \quad [\mathcal{K}\mathbf{n} \cdot \nabla T]_{\mathcal{I}} = 0. \quad (13)$$

The first condition says that the fluid velocity on the interface must match that of the solid. For an inviscid fluid this jump condition will only apply to the normal component the velocity since the fluid can slip along the interface. The second jump condition defines a balance of forces across the interface and states that the forces (surface traction) must balance if the interface has no mass. The third condition on the heat flux applies to problems with heat conduction; \mathcal{K} is the coefficient of thermal conductivity of the material.

2.3 A fluid-solid piston problem

In this section, we consider a one dimension problem that couples the solution of an inviscid compressible fluid and a linear elastic solid. At $t = 0$ the fluid occupies the region $x > 0$ and the solid the region $x < 0$. The interface between the fluid and solid is denoted as $x = F(t)$ with $F(0) = 0$. The fluid domain is $\Omega^F = \{(x, t) \mid t \geq 0, x \geq F(t)\}$. The solid domain is $\Omega^S = \{(x, t) \mid t \geq 0, x \leq F(t)\}$.

2.3.1 Solution for the fluid

The fluid satisfies the one-dimensional Euler equations for $(\mathbf{x}, t) \in \Omega^F$,

$$\begin{aligned} \rho_t + (\rho u)_x &= 0 \\ (\rho u)_t + (\rho u^2 + p)_x &= 0 \\ (\rho E)_t + (\rho E u + p u)_x &= 0 \\ \rho E &= \rho e + \frac{1}{2}\rho u^2 = \frac{p}{\gamma - 1} + \frac{1}{2}\rho u^2 \end{aligned}$$

with initial conditions (for a fluid initially at rest with constant density and pressure)

$$\rho(x, 0) = \rho_0, \quad u(x, 0) = 0, \quad p(x, 0) = p_0, \quad \text{for } x > 0$$

and boundary condition

$$u(x, t) = \dot{F}(t), \quad \text{for } x = F(t).$$

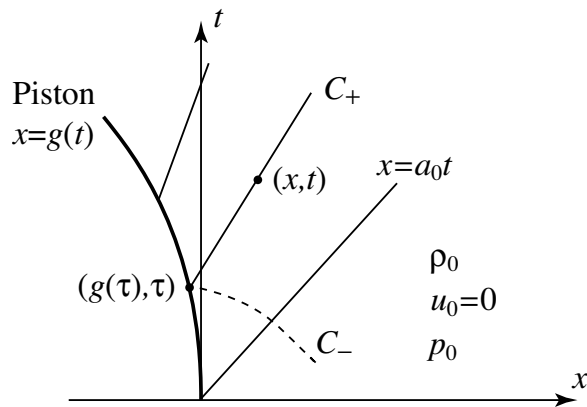


Figure 2: Exact solution for the fluid region with a moving boundary.

An x - t diagram for a one-dimensional piston is shown in Figure ?? . At time $t = 0$, an ideal gas with density ρ_0 , velocity $u_0 = 0$, pressure p_0 and sound speed $a_0 = (\gamma p_0 / \rho_0)^{1/2}$ occupies the channel to the right of the piston initially at $x = 0$. For $t > 0$ it is assumed that the piston moves according to the function $x = F(t)$, which for now we consider to be a known function. If $\dot{F}(t) < 0$ and $\ddot{F}(t) < 0$, then the piston recedes and no shocks form, and we may construct an exact solution using the method of characteristics as indicated in the figure. Since all C_- characteristics carry the same information from the uniform, undisturbed state for $x > a_0 t$, and thus the C_+ characteristics from the piston face are straight lines. For a given point (x, t) in the disturbed flow, the corresponding point $(F(\tau), \tau)$ on the piston following a C_+ characteristic is determined by

$$x - F(\tau) = \left[a_0 + \frac{\gamma + 1}{2} \dot{F}(\tau) \right] (t - \tau).$$

Once the parameter τ is found, the exact solution at (x, t) is given by

$$u = \dot{F}(\tau), \quad \frac{a}{a_0} = 1 + \frac{\gamma - 1}{2} \left(\frac{u}{a_0} \right), \quad \frac{p}{p_0} = \left(\frac{\rho}{\rho_0} \right)^\gamma = \left(\frac{a}{a_0} \right)^{2\gamma/(\gamma-1)}, \quad (14)$$

since the flow is isentropic (see Whitham [8]).

The flow is determined by the function $F(t)$, the position of the piston face. If this function is specified, then the exact solution is complete and this solution may be used to compare with numerical solutions.

2.3.2 Solution for the solid

The solid satisfies the equations of linear elasticity for $r < 0$, $t > 0$,

$$\begin{aligned} \rho_0^s \bar{u}_{tt} &= \sigma_r^s, \\ \sigma^s &= (\lambda + 2\mu) \bar{u}_r, \end{aligned}$$

which in one-dimension reduces to the second-order wave equation

$$\bar{u}_{tt} = \bar{a}_0^2 \bar{u}_{rr}, \quad (15)$$

$$\sigma^s = \rho_0^s \bar{a}_0^2 \bar{u}_r, \quad (16)$$

where \bar{a}_0 is the speed of compression waves in the solid,

$$\bar{a}_0^2 = \frac{\lambda + 2\mu}{\rho_0^s}. \quad (17)$$

The initial conditions are given as

$$\bar{u}(r, 0) = \bar{u}_0(r) \quad \text{for } r < 0,$$

$$\bar{v}(r, 0) = \bar{v}_0(r) \quad \text{for } r < 0,$$

where $\bar{v} = \partial_t \bar{u}$ is the solid velocity. The boundary condition is

$$\bar{u}(0, t) = F(t) \quad \text{for } t > 0. \quad (18)$$

Note that for linear elasticity the boundary condition is imposed at $r = 0$.

The general solution to these equations is of the form

$$\bar{u}(r, t) = f(r - \bar{a}_0 t) + g(r + \bar{a}_0 t) \quad (19)$$

where f and g are some unknown functions. Imposing the initial conditions implies

$$\begin{aligned} f(r) + g(r) &= \bar{u}_0(r), \quad \text{for } r < 0 \\ -\bar{a}_0 f'(r) + \bar{a}_0 g'(r) &= \bar{v}_0(r) \quad \text{for } r < 0. \end{aligned}$$

These two equations give $f(r)$ and $g(r)$ for $r < 0$

$$f(r) = \frac{1}{2} \left[\bar{u}_0(r) - \frac{1}{\bar{a}_0} \int_0^r \bar{v}_0(s) ds \right] \quad \text{for } r < 0, \quad (20)$$

$$g(r) = \frac{1}{2} \left[\bar{u}_0(r) + \frac{1}{\bar{a}_0} \int_0^r \bar{v}_0(s) ds \right] \quad \text{for } r < 0. \quad (21)$$

The initial conditions thus determine the full solution for $x + \bar{a}_0 t < 0$. Imposing the boundary condition at $r = 0$ gives

$$f(-\bar{a}_0 t) + g(\bar{a}_0 t) = F(t) \quad \text{for } t > 0$$

which defines $g(\xi)$ for $\xi > 0$,

$$g(\xi) = F(\xi/\bar{a}_0) - f(-\xi) \quad \text{for } \xi > 0 \quad (22)$$

since $f(-\xi)$ is known from (20).

Thus if $F(t)$ is a known function then the solution to the solid problem is given by (19) with $f(\xi)$ defined by (20) for $\xi < 0$ (f is only needed for negative argument) and $g(\xi)$ defined by (21) for $\xi < 0$ and (22) for $\xi > 0$.

2.3.3 Solution to the coupled fluid-solid problem

In the coupled problem, $F(t)$ is an unknown function. It is determined by imposing the traction boundary condition at the interface which states that the forces on the solid and the fluids at the interface have to match: (**check the sign**)

$$\sigma^s(0, t) = -p_0 \left[1 + \frac{\gamma - 1}{2a_0} \dot{F}(t) \right]^{2\gamma/(\gamma-1)} \quad (23)$$

From the definition (16) for σ^s and the condition $\bar{v}(0, t) = \dot{F}(t)$, it follows that f' and g' satisfy

$$\rho_0^s \bar{a}_0^2 [f'(-\bar{a}_0 t) + g'(\bar{a}_0 t)] = \sigma^s(0, t) \quad \text{for } t > 0, \quad (24)$$

$$-\bar{a}_0 f'(-\bar{a}_0 t) + \bar{a}_0 g'(\bar{a}_0 t) = \dot{F}(t) \quad \text{for } t > 0, \quad (25)$$

it follows that

$$f'(-\bar{a}_0 t) = \frac{1}{2} \left[\frac{\sigma^s(0, t)}{\rho_0^s \bar{a}_0^2} - \frac{\dot{F}(t)}{\bar{a}_0} \right] \quad \text{for } t > 0, \quad (26)$$

$$g'(\bar{a}_0 t) = \frac{1}{2} \left[\frac{\sigma^s(0, t)}{\rho_0^s \bar{a}_0^2} + \frac{\dot{F}(t)}{\bar{a}_0} \right] \quad \text{for } t > 0. \quad (27)$$

Note that $f'(\xi)$ is known for $\xi < 0$ from the derivative of (20) as

$$f'(r) = \frac{1}{2} \left[\bar{u}'_0(r) - \frac{1}{\bar{a}_0} \bar{v}_0(r) \right] \quad \text{for } r < 0 \quad (28)$$

Substituting (23) and (28) into (26) gives

$$\frac{p_0}{\rho_0^s \bar{a}_0^2} \left[1 + \frac{\gamma - 1}{2a_0} \dot{F}(t) \right]^{2\gamma/(\gamma-1)} + \frac{\dot{F}(t)}{\bar{a}_0} = - \left[\bar{u}'_0(-\bar{a}_0 t) - \frac{1}{\bar{a}_0} \bar{v}_0(-\bar{a}_0 t) \right] \quad \text{for } t > 0. \quad (29)$$

This is an implicit relation determining $\dot{F}(t)$ which we write as

$$\dot{F}(t) = \mathcal{F}(t; \bar{u}_0, \bar{v}_0). \quad (30)$$

This equation can be integrated in time to give $F(t)$ and the full solution the fluid-solid problem is thus known.

2.3.4 Initial conditions of a solid at rest

Consider the special case when the solid is initially at rest, $\bar{u}_0(r) = 0$ and $\bar{v}(r) = 0$. Then

$$\frac{p_0}{\rho_0^s \bar{a}_0^2} \left[1 + \frac{\gamma - 1}{2a_0} \dot{F}(t) \right]^{2\gamma/(\gamma-1)} = - \frac{\dot{F}(t)}{\bar{a}_0}. \quad (31)$$

Provided this equation has a real solution, $\dot{F}(t)$ will be constant, and F will vary linearly with t ,

$$F(t) = -\beta t \quad (32)$$

The solution for $\bar{u}(r, t)$ in this case will be (note $f(r) \equiv 0$, $g(r) \equiv 0$ for $r < 0$, and $g(r) = F(r/\bar{a}_0)$ for $r > 0$)

$$\bar{u}(r, t) = \begin{cases} -\beta(r/\bar{a}_0 + t) & \text{for } -\bar{a}_0 t < r < 0, \\ 0 & \text{for } r < -\bar{a}_0 t. \end{cases} \quad (33)$$

As a consistency check, we note that this is clearly a (weak) solution of the wave equation that satisfies the initial conditions and boundary conditions. In addition the stress is constant on the boundary $r = 0$.

2.3.5 Solid initial conditions chosen to give a specified fluid motion

Question: Can we define initial conditions for the fluid and solid so that the interface follows a given path?

Suppose we are given a desired interface motion such as $F(t) = -\frac{a}{p}t^p$, then from equation (29) we see that the initial conditions for the solid should satisfy

$$-\bar{u}'_0(-\bar{a}_0t) + \frac{1}{\bar{a}_0}\bar{v}_0(-\bar{a}_0t) = \frac{p_0}{\rho_0^s \bar{a}_0^2} \left[1 + \frac{\gamma-1}{2a_0} \dot{F}(t) \right]^{2\gamma/(\gamma-1)} + \frac{\dot{F}(t)}{\bar{a}_0} \quad (34)$$

$$\equiv G(t) \quad (35)$$

There are many solutions to this problem. For example, we could choose:

$$\bar{v}_0(x) = \bar{a}_0 G(-x/\bar{a}_0), \quad \text{for } x < 0, \quad (36)$$

$$\bar{u}_0(x) = 0 \quad (37)$$

2.3.6 Fluid-solid piston problem results

We solve the fluid-solid piston problem on the grid shown in figure 3. The solid domain on the left uses a single grid. The fluid domain uses two grids; a fixed background grid and a narrow grid on the interface. This narrow grid moves with the interface. It is recomputed at each time step using the hyperbolic grid generator.

We choose constant initial conditions for the fluid and solid as

$$\begin{aligned} \gamma &= 1.4, \quad \rho_0 = \gamma, \quad p_0 = 1, \quad a_0 = \sqrt{\gamma p_0 / \rho_0} = 1, \\ \lambda &= 1, \quad \mu = 1, \quad \rho^s = 1, \quad \bar{a}_0 = \sqrt{(\lambda + 2\mu) / \rho^s} = \sqrt{3}. \end{aligned}$$

The exact solution is given by equation (14) for the fluid and (33) for the solid. The interface moves at a constant velocity defined by equation (31) with

$$\begin{aligned} F(t) &= -\beta t, \\ \beta &\approx -0.3482883. \end{aligned}$$

Note that the interface instantaneously accelerates from rest to the constant velocity $-\beta$.

Figure 4 shows some results. We solve the fluid equations with the Godunov solver. The solid equations are solved with the SOS-NC method.

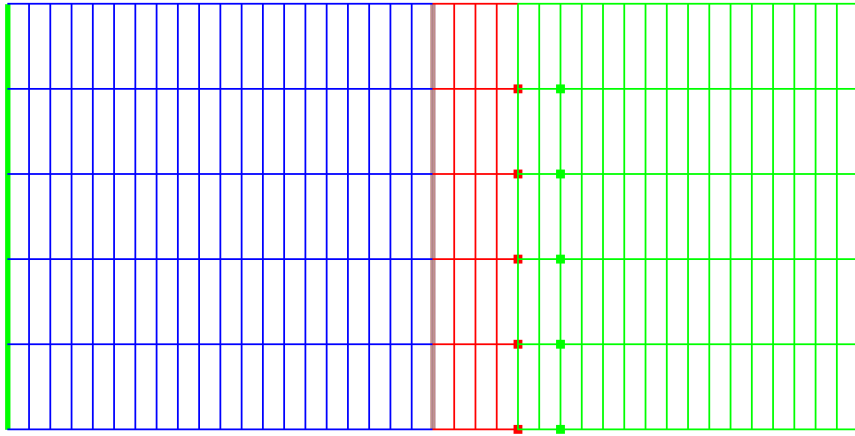


Figure 3: Grid for the fluid-solid piston problem.

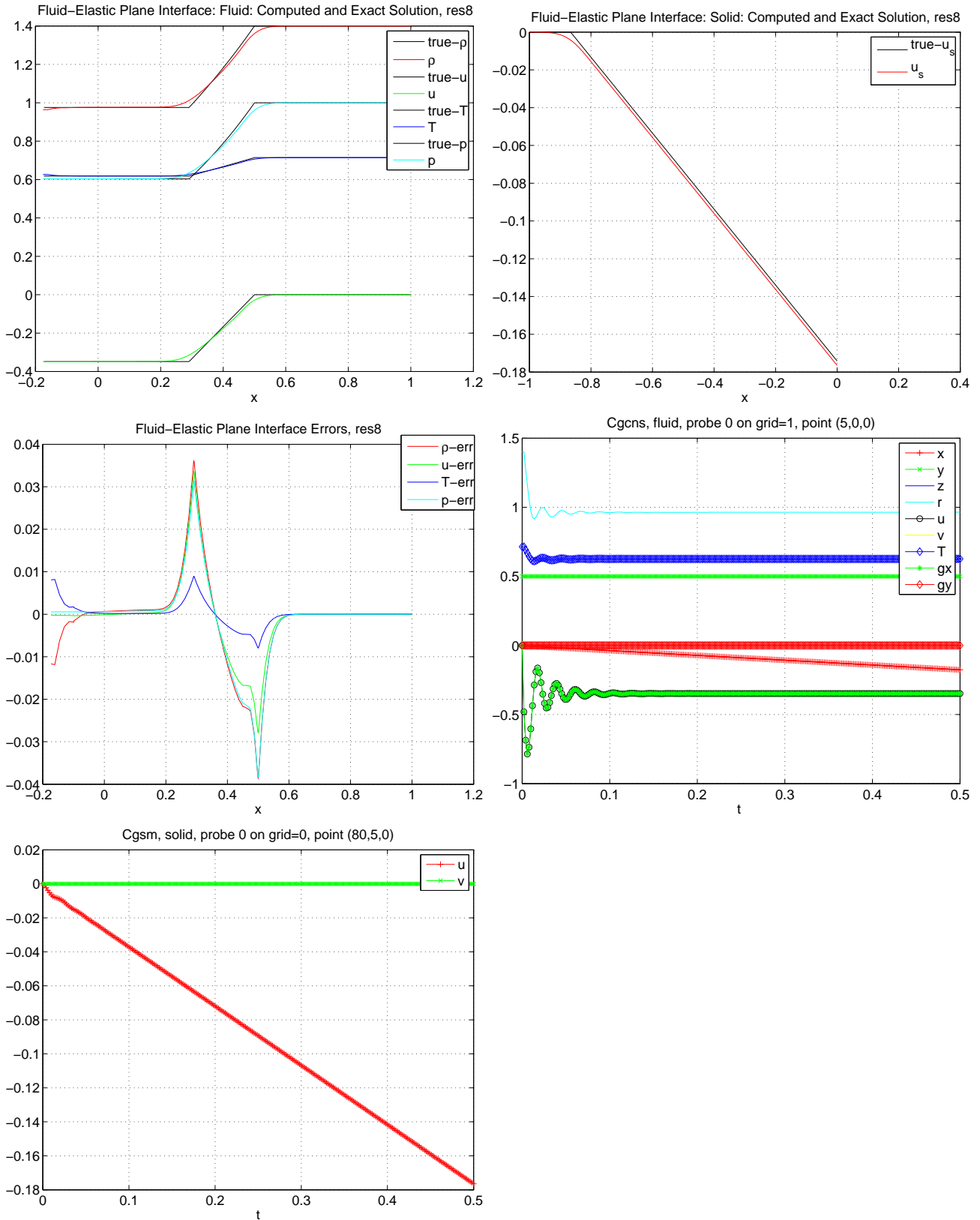


Figure 4: Fluid-solid piston. Solution at $t = 0.5$. Fluid (godunov), solid (SOS), res=8. Top-left: solution in the fluid. Top-right solution in the solid. Middle-left: errors in the fluid solution. Middle-right: The solution over time of the fluid properties at a point on the interface. Bottom-left : solid properties at a point on the interface.

2.4 The FSI-DCG numerical approach

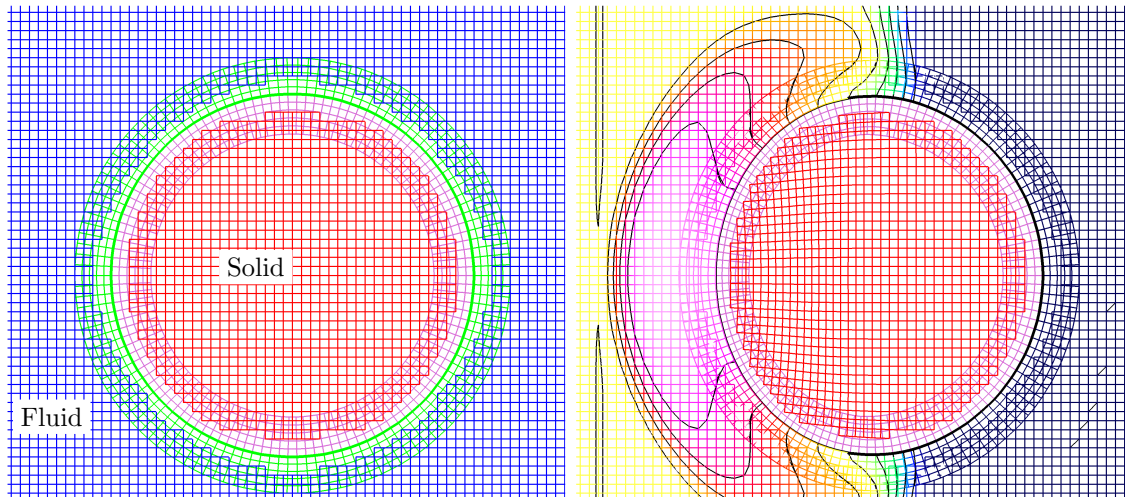


Figure 5: Left: a composite grid used in the FSI-DCG approach for a fluid-solid simulation. An overlapping grid covers the outer fluid domain (blue and green grids). A second overlapping grid covers the solid domain (red and pink grids). There are two deforming grids (green and pink) that match to the interface. Right: preliminary results from a simulation of a shock hitting an elastic solid showing the density in the fluid (plotted on the deformed fluid grid) and the deformation of the solid.

The deforming composite grid (DCG) approach for fluid-structure-interaction (FSI) problems is based on a mixed Eulerian/ALE formulation. We use the Eulerian description (8) on static (non-moving) grids and the equations for a general moving coordinate system (9) for moving and deforming grids. As discussed in section 2.1, the fluid-solid domain, Ω_t , is divided into fluid domains and solid domains. There can be any number of fluid and solid domains (see figure 1). Figure 5 shows the composite grid for a simple fluid-solid problem along with very preliminary results from a two-dimensional simulation of a shock hitting an elastic cylinder. One overlapping grid is used for the fluid domain. A second overlapping grid is used for the solid domain. Localized, curvilinear, deforming grids are used next to the deforming interface. Static grids are used in the remaining portions of the domain. As the interface changes over time, the deforming grid will also change to match the interface. The overlapping grid interpolation points will be updated at each time step to adjust for the motion of the interface grids.

For generation of the deforming grids we will begin by using our hyperbolic grid generator [4]. This grid generator is used at each time step to construct a new grid based on the current location of the interface and was used in the results presented in figure 5. The overlapping grid generator Ogen [3] is then called to update the interpolation points. There are also a variety of other approaches that have been used to define the motion of ALE grids; these include methods based on smoothing algorithms and those using evolution equations for the grid points, see for example [?]. We will investigate and compare some of these approaches which may provide grids that vary more smoothly in time compared to the hyperbolic technique.

3 Exit Plan

Using the results obtained from this 10 week feasibility study we have submitted a proposal to the DOE ASCR office [6] to obtain funding for further developing algorithms to model fluid-structure

interaction problems.

4 References

- [1] T. BELYTSCHKO, W. K. LIU, AND B. MORAN, *Nonlinear Finite Elements for Continua and Structures*, John Wiley and Sons, New York, 2005.
- [2] G. S. CHESHIRE AND W. D. HENSHAW, *Composite overlapping meshes for the solution of partial differential equations*, J. Comput. Phys., 90 (1990), pp. 1–64.
- [3] W. D. HENSHAW, *Ogen: An overlapping grid generator for Overture*, Research Report UCRL-MA-132237, Lawrence Livermore National Laboratory, 1998.
- [4] ———, *The Overture hyperbolic grid generator, user guide, version 1.0*, Research Report UCRL-MA-134240, Lawrence Livermore National Laboratory, 1999.
- [5] ———, *A high-order accurate parallel solver for Maxwell's equations on overlapping grids*, SIAM Journal on Scientific Computing, 28 (2006), pp. 1730–1765.
- [6] W. D. HENSHAW AND J. W. BANKS, *Domain-adaptive high-order accurate algorithms for PDEs in moving geometry*, Research Report LLNL-PROP-410221, Lawrence Livermore National Laboratory, 2009. Proposal submitted to ASCR, DOE Office of Science.
- [7] W. D. HENSHAW AND K. K. CHAND, *A composite grid solver for conjugate heat transfer in fluid-structure systems*, J. Comput. Phys., (2009). To appear.
- [8] G. B. WHITHAM, *Linear and Nonlinear Waves*, John Wiley and Sons, New York, 1974.